Structure and Conformational Properties of N-Pentafluorosulfur(sulfuroxide difluoride imide) $SF_5N{=}S(O)F_2$: Vibrational Analysis, Gas Electron Diffraction, and Quantum Chemical Calculations

Rosa M. S. Alvarez,[†] Edgardo H. Cutin,[†] Rüdiger Mews,[‡] and Heinz Oberhammer*[,§]

Instituto de Química Física, Facultad de Bioquímica, Química y Farmacia, Universidad Nacional de Tucumán, San Lorenzo 456, (4000) Tucumán, República Argentina, Institut für Anorganische und Physikalische Chemie, Universität Bremen, 28334 Bremen, Germany, and Institut für Physikalische und Theoretische Chemie, Universität Tübingen, 72076 Tübingen, Germany

Received: December 18, 2006; In Final Form: January 18, 2007

The molecular structure and conformational properties of *N*-pentafluorosulfur(sulfuroxide difluoride imide), $SF_5N{=}S(O)F_2$, have been studied by vibrational spectroscopy (IR (gas) and Raman (liquid)), by gas electron diffraction (GED), and by quantum chemical calculations (MP2 and B3LYP with (6-31G(d) and 6-311+G-(2df) basis sets). According to GED, the prevailing conformer possesses a syn structure ($N{-}SF_5$ bond synperiplanar with respect to the bisector of the SF_2 group). Splitting of the symmetric $N{=}S{=}O$ stretching vibration in gas and liquid spectra demonstrates the presence of a second conformer (11(5)%) with anticlinal orientation of the $N{-}SF_5$ bond according to quantum chemical calculations. The geometric structure, conformational properties, and vibrational frequencies are well reproduced by quantum chemical calculations.

Introduction

Gas electron diffraction (GED) and/or microwave spectroscopy for sulfurdifluoride imides of the type $RN{=}SF_2$ with $R{=}$ Cl,[1] CF_3,[2,3] SF_5,[4] CN,[5] FC(O),[6] $CF_3C(O)$,[7] and SFO_2[8] resulted in the presence of a syn configuration around the N═S bond with the substituent R synperiplanar with respect to the bisector of the SF_2 group (see Chart 1).

This sterically unfavorable configuration with the electron lone pairs of nitrogen and sulfur eclipsing each other is stabilized by orbital interactions of the two lone pairs with the opposite S−F and N−R antibonding σ^* orbitals, respectively (anomeric effects). No such anomeric effects are present in the anti form. Similarly, for sulfuroxidedifluoride imides of the type $RN{=}S(O)F_2$ with R═Cl,[9] CN,[10] and SFO_2,[8] only the syn form (R synperiplanar with respect to the SF_2 bisector) has been observed (Chart 2). Furthermore, both N−C bonds in *NN*′-carbonyl-bis-(sulfuroxidedifluoride imide, $O{=}C(N{=}S(O)F_2)_2$, are oriented syn relative to the bisector of the SF_2 group.[11] In a recent conformational study for *N*-fluoroformyl(sulfuroxidedifluoride imide), $FC(O)N{=}S(O)F_2$, however, a small amount of 14(8)% of a conformer with anticlinal orientation around the N═S bond was observed.[12] This study was complicated by the presence of one or two more conformers with different orientation of the FC(O) group around the N−C bond. In the course of structural and conformational investigations of sulfur imide and sulfuroxide imide compounds we now report the results for *N*-pentafluorosulfur(sulfuroxide difluoride imide), $SF_5N{=}S(O)F_2$, as derived by vibrational spectroscopy, GED, and quantum chemical calculations. The first synthesis of this compound, some vibrational transitions and ^{19}F NMR data have been reported by Höfer and Glemser.[13]

CHART 1

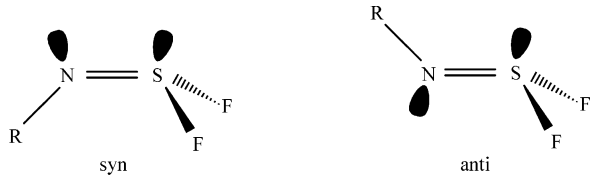

CHART 2

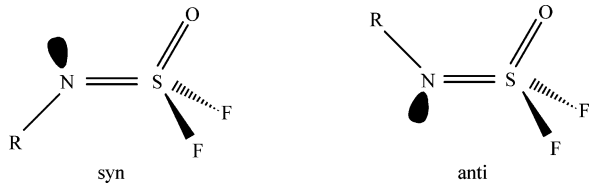

Quantum Chemical Calculations. In a first step, geometry optimizations for the syn conformation were performed using the B3LYP method and MP2 approximation with small (6-31G-(d)) and large (6-311+G(2df)) basis sets. Both methods with small basis sets result in a geometry with C_1 symmetry. The torsional orientation of the SF_5 group is intermediate between eclipsing and staggering the N═S bond. Dihedral angles $\phi(F_{bas}{-}S{-}N{=}S)$ of 24.2° (B3LYP) and 15.1° (MP2) were derived (F_{bas} designates one of the fluorine atoms in the basal plane of the SF_5 group, F_{ap} is used for the unique apical fluorine atom). Both methods with large basis sets, however, predict structures with C_S symmetry and exactly eclipsing SF_5 groups ($\phi(F_{bas}{-}S{-}N{=}S) = 0°$). In all cases the potential function for internal rotation around the N−S bond is very flat near the eclipsed orientation and the calculated barrier to internal rotation which occurs for staggered orientation is low (0.16 kcal/mol from B3LYP/6-31G-(d) and 0.82 kcal/mol from MP2/6-311+G(2df)).

In the second step, geometry optimizations for different fixed torsional angles around the N═S bond from synperiplanar

* To whom correspondence should be addressed. E-mail: heinz.oberhammer@uni-tuebingen.de.
† Universidad Nacional de Tucuman.
‡ Universität Bremen.
§ Universität Tübingen.

10.1021/jp068671s CCC: $37.00
Published on Web 02/23/2007

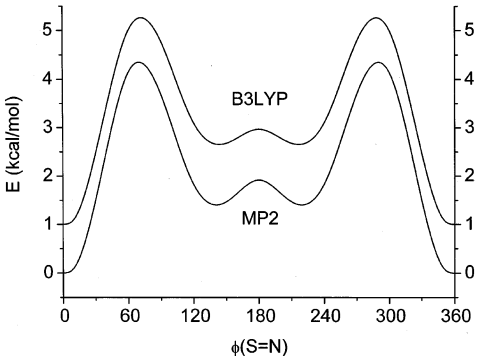

Figure 1. Calculated Potential curve for internal rotation around the S=N bond. ϕ(S=N) = 0° corresponds to the syn conformer. Calculations were performed with 6-31G(d) basis sets. The B3LYP curve is shifted by 1 kcal/mol relative to the MP2 curve.

TABLE 1: Calculated Torsional Angles ϕ(N=S), Relative Energies $\Delta E = E$(anti) − E(syn) and Gibbs Free Energies ΔG^0 for Anti Conformer in kcal/mol

	B3LYP/sb[b]	B3LYP/lb[c]	MP2/sb[b]	MP2/lb[c,d]
ϕ(N=S)[a]	140.7°	141.5°	138.4°	140.2°
$\Delta E = E$(anti) − E(syn)	1.66	1.56	1.41	1.30
$\Delta G^0 = G^0$(anti) − G^0(syn)	0.90	1.01	0.82	0.75
% anti	18	16	20	22

[a] ϕ(N=S) = 0° for syn conformer. [b] sb = small basis sets, 6-31G(d). [c] lb = large basis sets, 6-311+(2df). [d] Corrections between ΔE and ΔG^0 taken from B3LYP/lb calculation.

orientation (ϕ(N=S) = 0°) to antiperiplanar orientation (ϕ(N=S) = 180°) were performed with both methods and small basis sets. The calculated potential functions for internal rotation around the N=S double bond (Figure 1) possess minima for anticlinal orientation of the N−S single bond relative to the SF_2 bisector, in addition to the global minimum for the syn form. The geometries of the anti form were fully optimized with both methods and small and large basis sets. The calculated torsional angles ϕ(N=S), relative energies ΔE, and Gibbs free energies ΔG^0 for the anti conformer are summarized in Table 1. ΔG^0 values account also for the higher multiplicity ($m = 2$) of the anti conformer. All computational methods predict an anticlinal structure with ϕ(N=S) around 140° with the N−S bond staggering the S=O and one S−F bond of the $S(O)F_2$ group. The population of this conformer at room temperature is predicted to be between 16 and 22%. The geometric parameters of the syn form derived with B3LYP and MP2 method and large basis sets are included in Table 3 together with the experimental values. The B3LYP/6-311+G(2df) force fields were used to calculated vibrational amplitudes (see Table 4) and vibrational corrections $\Delta r = r_{h1} - r_a$ with the method of Sipachev.[14] All quantum chemical calculations were performed with the GAUSSIAN03 program set.[15]

Vibrational Spectra. The observed IR (gas) and Raman (liquid) spectra have been assigned on the basis of their calculated vibrational frequencies and intensities (Table 2). Furthermore, characteristic wavenumbers of the $N{=}S(O)F_2$ moiety in the related molecules $FSO_2NS(O)F_2$,[16] $NCNS(O)F_2$,[17] and $FCONS(O)F_2$[18] have been taken into account. For assignment of the modes belonging to the SF_5N group additional calculations (MP2) were performed for SF_5NCO and SF_5NSF_2, for which no experimental data are available.

Observed and calculated wavenumbers, together with a tentative assignment for the $3N - 6 = 27$ normal modes expected for $SF_5NS(O)F_2$ are listed in Table 2. In general, good agreement exists between the experimental and calculated values derived by the different approximations (B3LYP/6-311+G(2df); MP2/6-31+G(d)). Some experimental wavenumbers are reproduced closer by the B3LYP method, others by the MP2 approximation. Strong couplings between some fundamental modes involving both SF_5N and $N{=}S(O)F_2$ moieties of the molecule are evident from the calculated vibrational behavior.

TABLE 2: Assignments of Fundamental Modes and Experimental and Calculated Wavenumbers (cm^{-1}) for $SF_5N{=}S(O)F_2$

mode	approximate description[a]	IR[b,c]	Raman[c,d]	B3LYP 6-311+ G(2df)	MP2 6-31+ G(d)
υ_1	N=S=O asym. stretch.	1446 s	1437 m	1417	1452
υ_2	N=S=O sym. stretch.	1277 s	1272 m	1251	1273
υ_3	SF_4 asym. stretch.	918 vs	917 w	887	967
υ_4	SF_4 asym. stretch.	918 vs	917 w	877	965
υ_5	$S-F_{ap}$ stretch.	881 m	898 m	868	929
υ_6	SF_2 asym. stretch.	857 m	854 w	809	855
υ_7	SF_2 sym. stretch.	808 s	799 m	764	811
υ_8	SF_4 sym. stretch.	702 m	709 vs	671	700
υ_9	SF_4 sym. stretch.	655 w	646 m	591	649
υ_{10}	S−N stretch.	613 sh	617 m	614	639
υ_{11}	SF_5 sym. def.	591 s	588 m	582	595
υ_{12}	SF_5 asym. def.	570 m		574	565
υ_{13}	$S(O)F_2$ sym. def.	570 m		564	553
υ_{14}	SF_5 asym. def.		504 w	541	531
υ_{15}	NSF_5 def.		504 w	524	517
υ_{16}	NSF_5 def.	470 vw	475 w	476	465
υ_{17}	$S(O)F_2$ def. (rocking)	445 vw	454 m	455	442
υ_{18}	$S(O)F_2$ def. (scissor)		411 m	429	418
υ_{19}	NSF_5 def.		381 w	389	389
υ_{20}	NSF_5 asym. def.		328 s	361	352
υ_{21}	NSF_5 asym. def.		328 s	337	334
υ_{22}	$S(O)F_2$ def. (wagging)		304 w	313	312
υ_{23}	$S(O)F_2$ def. (twisting)		278 sh	255	247
υ_{24}	NSF_5 def.		266 s	251	245
υ_{25}	SNS def.			125	140
υ_{26}	SNSO torsion		84 m	76	84
υ_{27}	FSNS torsion			33	35

[a] stretch. = stretching; def. = deformation; sym. = symmetric; asym. = antisymmetric. [b] Gas phase. [c] Relative intensities: vw = very weak; w = weak; m = medium; s = strong; vs = very strong; sh = shoulder. [d] Liquid phase.

TABLE 3: Experimental and Calculated Geometric Parameters for Syn Conformer of $SF_5N{=}S(O)F_2$

	GED[a]		MP2[b]	B3LYP[b]
N=S1	1.478(8)	p1	1.482	1.488
N−S2	1.656(9)	p2	1.680	1.698
S=O	1.385(4)	p3	1.412	1.413
$(S-F)_{mean}$	1.560(1)	p4	1.572	1.587
S1−F1/S1−F2	1.541[c]		1.553	1.566
S2−F3	1.566[c]		1.578	1.594
S2−F4	1.582[c]		1.594	1.610
S2−F5/S2−F7	1.568[c]		1.580	1.596
S2−F6	1.556[c]		1.560	1.583
S1=N−S2	132.7(10)	p5	129.6	130.4
N=S1=O	120.3(14)	p6	118.8	118.3
N=S1−F1	109.6(7)	p7	111.8	112.2
O=S1−F1	108.8(12)	p8	108.6	108.5
F1−S1−F2	96.9(18)		94.6	94.4
$F_{ap}-S2-F_{bas}$	87.8(3)	p9	88.7	88.6
Tilt (SF_5)[d]	2.8(10)	p10	2.4	2.6
$\phi(F_{bas}-S2-N=S1)$[e]	20.5(25)	p11	0.0	0.0

[a] r_{h1} distances (Å) and angles (deg) with 3σ uncertainties. For atom numbering see Figure 3. [b] 6-311+G(2df) basis sets. [c] Difference to mean S−F distance set to calculated (MP2) difference. [d] Tilt between $S-F_{ap}$ and S−N bond, away from oppposite SF_2 group. [e] Torsional angle of SF_5 group around S1−N bond; $\phi = 0$ corresponds to eclipsed orientation of $S-F_{bas}$ relative to S=N bond.

TABLE 4: Interatomic Distances and Experimental and Calculated Vibrational Amplitudes[a]

	distance	ampl. (GED)		ampl. (MP2)[b]
S═O	1.39	0.034[c]		0.034
N═S1	1.48	0.038[c]		0.038
S−F	1.54−1.58	0.045(2)	*l*1	0.042
N−S2	1.66	0.048[c]		0.048
F···F	2.21−2.23	0.061(3)	*l*2	0.072
N···F	2.23−2.43	0.081[c]		0.081
F1···F2	2.34	0.068[c]		0.068
O···F1	2.38	0.064[c]		0.064
N···F1	2.47	0.068[c]		0.068
N···O	2.48	0.076(21)	*l*3	0.056
F1···F4	2.78	0.186[c]		0.186
F2···F7	2.78	0.377[c]		0.377
S1···F4	2.80	0.136 (14)	*l*4	0.143
S1···S2	2.86	0.055(6)	*l*5	0.053
S1···F7	3.07	0.184(23)	*l*6	0.204
F2···F4	3.07	0.239[c]		0.239
F4···F6	3.13	0.055(11)	*l*7	0.054
N···F3	3.21	0.055(11)	*l*7	0.057
S2···F1	3.34	0.136(14)	*l*4	0.125
S1···F5	3.46	0.184(23)	*l*6	0.189
F1···F5	3.57	0.389[c]		0.389
S1···F6	3.67	0.071(13)	*l*8	0.091
F1···F7	3.80	0.136(14)	*l*4	0.141
S2···O	4.08	0.076(20)	*l*3	0.061
O1···F4	4.15	0.136(14)	*l*4	0.142
F2···F4	4.21	0.136(14)	*l*4	0.141
O···F7	4.27	0.136(14)	*l*4	0.143
S1···F3	4.36	0.071(13)	*l*8	0.077
F2···F5	4.41	0.223[c]		0.223
O···F5	4.47	0.196[c]		0.196
F1···F6	4.54	0.136(14)	*l*4	0.141
O···F6	4.58	0.184(23)	*l*6	0.180
F1···F3	4.60	0.178[c]		0.178
O···F3	5.72	0.071(13)	*l*8	0.074

[a] Values in Å, error limits are 3σ values. For atom numbering see Figure 3. [b] 6-31G* basis sets. [c] Not refined.

However, in Table 2 all modes are defined as pure vibrations of a single group, in order to allow simpler group wavenumbers correlations.

The characteristic bands centered at 1446 and 1277 cm^{-1} in the IR spectrum of the gas phase and at 1437 and 1272 cm^{-1} in the Raman spectrum of the liquid phase are straightforwardly assigned to the antisymmetric and symmetric N═S═O stretching modes, respectively, in fair agreement with the data reported for the related molecules $FSO_2NS(O)F_2$,[16] $NCNS(O)F_2$,[17] and $FCONS(O)F_2$.[18] The band assigned to the N═S═O symmetric mode in the IR (gas) spectrum (1277 cm^{-1}) shows a well-defined shoulder at lower wavenumbers (at approximately 1263 cm^{-1}) demonstrating the presence of a second conformer, which possesses anticlinal orientation of the N−S bond with respect to the SF_2 group, according to the theoretical calculations. The relative areas together with the ratio of the calculated intensities for N═S═O symmetric stretching vibration for the syn and anti conformers (MP2/6-31+G(d)) results in a contribution of the anti form of 11(5)%. The estimated error limit includes uncertainties in the measured relative areas and in the calculated intensities. In the Raman spectrum, a weak band centered at 1255 cm^{-1}, close to the 1272-cm^{-1} band with medium intensity, is assigned to the counterpart of the anticlinal conformer in the liquid phase. These assignments are supported by theoretical calculations, which predict the N═S═O symmetric stretching mode for the anti form to be shifted to lower wavenumbers by 23 cm^{-1} (B3LYP) or 30 cm^{-1} (MP2), compared to that for the main conformer.

The S−F stretching modes of the SF_5 group can be rationalized in terms of four complex vibrations involving the four $S-F_{bas}$ bonds and one vibration corresponding to the $S-F_{ap}$ bond. In the basal vibrations, a pair of S−F bonds stretches out-of-phase with respect to the stretching of the other two S−F bonds resulting in two antisymmetric and one symmetric fundamental mode defined with respect to the symmetry plane. The fourth complex vibration is interpreted as in-phase stretching of the basal S−F bonds. The antisymmetric stretching modes ($\nu(SF_4)$ asym. stretch.) are calculated at 887 and 877 (B3LYP/6-311+G(2df)) and 967 and 965 cm^{-1} (MP2/6−31+G(d)). Similar values were obtained for SF_5NCO and FS_5NSF_2 at the same levels of calculations. The experimental IR (gas) spectrum shows only a single, very strong and broad signal at 918 cm^{-1}, and the Raman (liquid) spectrum possesses a weak and broad band at 917 cm^{-1}, which are assigned to these two SF_5 modes. The remaining out-of-phase S−F basal stretching mode ($\nu(SF_4)$ sym. stretch.) is assigned to the weak signals observed at 655 (IR) and 646 cm^{-1} (Raman), very close to the calculated MP2/6-31+G(d) value of 649 cm^{-1}. The fully symmetric vibration with all four basal S−F bonds stretching in-phase is predicted to be the most intense Raman band at 671 and 700 cm^{-1} (B3LYP and MP2, respectively), and it is assigned, in accordance, to the strongest Raman signal centered at 709 cm^{-1} (702 cm^{-1} in IR). Finally, the stretching mode of the apical $S-F_{ap}$ bond is assigned at 881 (IR) and 898 cm^{-1} (Raman).

Two additional S−F stretching modes are expected for this molecule corresponding to the $S(O)F_2$ group. The out-of-phase and in-phase vibrations of the S−F bonds are defined in Table 2 as SF_2 antisymmetric and SF_2 symmetric stretching modes, respectively. The assignment of the observed IR band at 857 cm^{-1} to the antisymmetric mode (854 cm^{-1} in Raman) and the band at 808 cm^{-1} (799 cm^{-1}, Ra) to the symmetric fundamental is supported by the reported values and by the relative Raman intensities for $FC(O)NS(O)F_2$ (876 and 815 (IR) and 885 and 817 cm^{-1} (Ra)) and $NCNS(O)F_2$ (868 (asym. stretch., IR) and 869 and 793 cm^{-1} (Ra)). In all these cases, the Raman signals corresponding to the symmetric SF_2 mode are stronger than that of the antisymmetric mode.

The S−N single bond stretching mode is observed in the IR as a shoulder at approximately 613 cm^{-1}, and as medium intensity Raman band at 617 cm^{-1}, in very good agreement with the value calculated with the B3LYP method (614 cm^{-1}). All the calculations for this molecule and for the related SF_5NSF_2 and SF_5NCO predict this vibration to be strongly coupled with the $S-F_{ap}$ stretching, which would suggest an alternative definition of the modes ν_5 and ν_{10} in Table 2 as $F_{ap}-S-N$ out-of-phase and in-phase stretching modes, respectively.

The assignment of the deformation modes belonging to the $N{=}S(O)F_2$ shows a very good correlation with the reported value for related molecules, except for the wagging vibration for which discrepancies are observed.

GED. The experimental radial distribution function (RDF) has been calculated by Fourier transformation of the modified molecular intensities using an artificial damping function $\exp(-\gamma s^2)$ with $\gamma = 0.0018$ $Å^{-2}$. Comparison of the experimental RDF with calculated curves for the syn and anti conformer (Figure 2) demonstrates that the syn conformer is the prevailing form. The calculated RDFs for the two conformers differ only slightly in the distance range from 2.7 to 4 Å. On the basis of the quantum chemical calculations, the presence of a mixture of syn and anti conformers was assumed in the least-squares fitting of the molecular intensities. For the syn form the $SN{=}S(O)F_2$ moiety was constrained to C_s symmetry and an effective

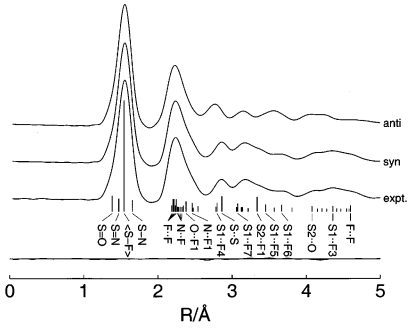

Figure 2. Experimental and calculated radial distribution functions and difference curve for syn conformer only. Vertical bars indicate interatomic distances for syn conformer.

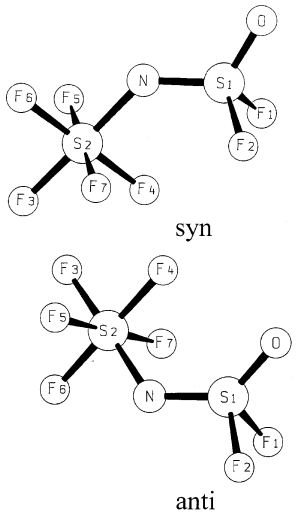

Figure 3. Molecular models with atom numbering for syn (above) and anti (below) conformers.

torsional angle around the N−S bond, $\phi(F_{bas}-S2-N=S1)$, was introduced to account for the large amplitude torsional vibration. For atom numbering, see Figure 3. A mean S−F bond length was refined and the differences between individual S−F distances and the mean distance were constrained to the calculated (MP2/6-311+G(2df)) values. The distortion of the F−S2−F angles from C_{4v} symmetry was described by a tilt angle between the S−N and S−F_{ap} bonds. Vibrational amplitudes were collected in groups and amplitudes, which either caused large correlations with geometric parameters or which are badly determined in the GED analysis, were constrained to calculated values. For the anti conformer all bond lengths and bond distances were tied to those of the syn form using the calculated differences and torsional angles around the N−S and N═S bonds were set to MP2 values. Similarly all vibrational amplitudes were constrained to calculated values. With these assumptions eleven geometric parameters (p1 to p11) and eight vibrational amplitudes ($l1$ to $l8$) for the syn conformer were refined independently. Four correlation coefficients had absolute values larger than 0.6: p2/p7 = 0.69, p6/p8 = −0.69, p1/$l1$ = 0.83, and p2/$l1$ = −0.80. Additional refinement of the torsional angle around the N═S bond, ϕ(N═S), resulted in a value of 2.3 ± 4.2° with no improvement of the R factor.

Least-squares refinements with different and fixed contributions of the anti form were performed. The best fit of the experimental intensities with an overall agreement factor of 3.53% is obtained for zero contribution of the anti form. The R factor increases very slowly with increasing anti contribution. The uncertainty derived by the Hamilton method for a significance level of 0.05 is 16%.[19] Final geometric parameters of the syn conformer are summarized in Table 3 together with the calculated values. Experimental and calculated vibrational amplitudes are given in Table 4.

TABLE 5: Orbital Interaction Energies (in kcal/mol) of Lone Pairs Lp(N) and Lp(S) with Vicinal σ^* Orbitals for Syn and Anti Conformers of $SF_5N{=}SF_2$ and $SF_5N{=}S(O)F_2$, Derived from MP2/6-31G(d) Wavefunctions

orbital interaction	$SF_5N{=}SF_2$ syn	$SF_5N{=}SF_2$ anti	$SF_5N{=}S(O)F_2$ syn	$SF_5N{=}S(O)F_2$ anti
lp(N) → σ^*(S-F1)	9.9	5.2	7.7	
lp(N) → σ^*(S-F2)	9.9	5.2	7.7	9.0
lp(N) → σ^*(S═O)			8.2	18.3
lp(S) → σ^*(N-S)	10.4			
∑ anomeric effects	30.2	10.4	23.6	27.3

Discussion

Analyses of IR (gas) and Raman (liquid) spectra result for both, gaseous and liquid phases, in a mixture of two conformers, 89(5)% with synperiplanar orientation of the N−S bond relative to the SF_2 group and 11(5)% with anticlinal orientation. The presence of the anti form is not observed in the GED analysis, but a contribution of up to 16% cannot be excluded by this method. Quantum chemical calculations predict a slightly higher contribution of the anti conformer of 16 to 22%.

As mentioned in the Introduction, the sterically unfavorable syn form in sulfurdifluoride imides $RN{=}SF_2$ is stabilized by orbital interactions of the nitrogen and sulfur electron lone pairs with vicinal σ^* antibonding orbitals. A natural bond orbital (NBO) analysis of the MP2/6-31G(d) wave function of $SF_5N{=}SF_2$ results in interaction energies (see Table 5) of 19.8 kcal/mol between the nitrogen lone pair and the two σ^*(S−F) orbitals and of 10.4 kcal/mol between the sulfur lone pair and the σ^*(N−S) orbital. The overall stabilization of the syn structure due to these anomeric effects amounts to 30.2 kcal/mol. The calculations predict also a stable anti structure of this sulfurimido compound with a relative energy of 7.2 kcal/mol. In this sterically more favored conformer the orbital interaction energy between the nitrogen lone pair and the σ^*(S−F) orbitals is only 10.4 kcal/mol.

In sulfuroxidedifluoride imides $RN{=}S(O)F_2$ different anomeric effects are present. In these compounds only the nitrogen lone pair participates in orbital interactions with vicinal S−F and S═O antibonding orbitals. Whereas experiments and quantum chemical calculations result in a higher energy of the anti form than that of the syn conformer, the stabilization due to orbital interactions is stronger in the anti structure (27.3 kcal/mol) than in the syn structure (23.6 kcal/mol). Anomeric stabilization of the anti form is dominated by the high interaction energy between the nitrogen lone pair and the σ^*(S═O) orbital of 18.3 kcal/mol. This interaction is considerably smaller in the syn form and no such interaction is present in the sulfuroxide imido compounds. From the overall stabilization energies of the syn and anti form of $SF_5N{=}S(O)F_2$ and from the relative total energies (see Table 1), we conclude that the syn form in which the N−S bond staggers the two S−F bonds of the $S(O)F_2$ group is sterically favored with respect to the anti conformer, in which the N−S bond staggers the S═O bond and one S−F bond. Thus, anomeric effects rationalize the different conformational properties of sulfurdifluoride imides and sulfuroxidedifluoride imides. Whereas no anti conformers have been observed so far for the sulfur imide derivatives, anti conformers

TABLE 6: Important Skeletal Geometric Parameters of Some Sulfuroxidedifluoride Imides $Rn{=}S(O)F_2$ and the Analogous Sulfurdifluoride Imides

compound	N=S	S=O[a]	S−F[b]	R−N=S
$SF_5N{=}S(O)F_2$[c]	1.478(8)	1.385(4)	1.541(1)	132.7(10)
$FC(O)N{=}S(O)F_2$[d]	1.469(10)	1.395(5)	1.534(3)	121.5(17)
$ClN{=}S(O)F_2$[e]	1.484(7)	1.394(3)	1.548(3)	114.7(8)
$SFO_2N{=}S(O)F_2$[f]	1.475(5)	1.392(5)	1.529(3)	125.9(8)
$SF_5N{=}SF_2$[g]	1.470		1.603	141.9
$FC(O)N{=}SF_2$[h]	1.479(4)		1.586(2)	126.7(11)
$ClN{=}SF_2$[i]	1.476(4)		1.596(2)	120.0(2)
$SFO_2N{=}SF_2$[f]	1.487(5)		1.575(3)	129.9(8)

[a] In S(O)F2 group. [b] In S(O)F2 or SF2 groups. [c] This work. [d] Reference 12. [e] Reference 9. [f] Reference 8. [g] Reference 4. [h] Reference 6. [i] Reference 1.

are observed for some sulfuroxide imide compounds such as $SF_5N{=}S(O)F_2$ and $FC(O)N{=}S(O)F_2$.

Table 6 compares important skeletal parameters of some sulfuroxide imide compounds with those of analogous sulfur imide derivatives. Surprisingly, the N=S bond length does not depend on the sulfur oxidation number, the mean value in the S(VI) compounds (1.477 Å) is equal to that in the S(IV) derivatives (1.478 Å). The S−F bond distances, however, show the expected behavior. The mean value increases from 1.538 Å in the S(VI) derivatives to 1.590 Å in the S(IV) compounds. The nitrogen bond angle R−N=S strongly depends on the substituent R. In the sulfuroxide imido compounds it increases from 114.7(8)° for R=Cl to 132.7(10)° for $R{=}SF_5$. This angle increases in the S(IV) derivatives by about 4−9°.

Experimental Section

$SF_5N{=}S(O)F_2$ was obtained according the method reported in the literature.[13] The compound was purified by repeated vacuum distillations. Since slow decomposition occurs at room temperature, the sample was stored and transported in liquid nitrogen.

The gas IR spectrum at 5 Torr was recorded between 4000 and 400 cm^{-1} (resolution 2 cm^{-1}) with an FT IR Perkin-Elmer Paragon 500 spectrometer, using a gas cell equipped with KBr windows. Raman spectra of the liquid between 4000 and 50 cm^{-1} were obtained using a Jobin Yvon V1000 spectrometer equipped with an argon ion laser (Spectra Physics model 165) and radiation of 514.5 nm (Ar^+) was used for excitation. The liquid samples were handled in glass capillaries at room temperature.

GED intensities were recorded with a KD-G2 Gasdiffraktograph[20] at 25 and 50 cm nozzle-to-plate distances and with an accelerating voltage of about 60 kV. The electron wavelength was derived from ZnO powder diffraction patterns. The sample was kept at −50 °C, and the inlet system and nozzle were at room temperature. The photographic plates (Kodak Electron Image Plates, 18 × 13 cm) were analyzed with an Agfa Duoscan HiD scanner and total scattering intensity curves were obtained using the program SCAN3.[21] Averaged experimental molecular intensities in the ranges $s = 2-18$ and $8-35$ $Å^{-1}$ in steps of $\Delta s = 0.2$ $Å^{-1}$ ($s = (4\pi/\lambda)\sin\theta/2$, where λ is the electron wavelength and θ is the scattering angle) are shown in Figure 4.

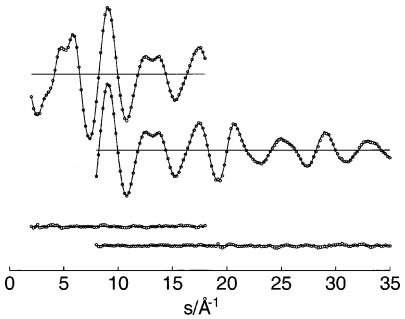

Figure 4. Experimental (dots) and calculated (full line) molecular intensities for long (above) and short nozzle-to-plate distances (below) and residuals.

Acknowledgment. Financial support by the Volkswagen Stiftung (I/78 724) and the Deutsche Forschungsgemeinschaft is gratefully acknowledged. R.M.S.A. and E.H.C. thank UNT and CONICET, R. Argentina for financial support. We thank Professor Carlos O. Della Védova, Universidad Nacional de La Plata, for recording Raman spectra.

References and Notes

(1) Haase, J.; Oberhammer, H.; Zeil, W.; Glemser, O.; Mews, R. *Z. Naturforsch.* **1970**, *23A*, 153.

(2) Karl, R. R.; Bauer, S. H. *Inorg. Chem.* **1975**, *14*, 1859.

(3) Trautner, F.; Christen, D.; Mews, R.; Oberhammer, H. *J. Mol. Struct.* **2000**, *525*, 135.

(4) White, R. M.; Baily, S. R.; Graybeal, J. D. M.; Trasher, J. S.; Palmer, M. H. *J. Mol. Spectrosc.* **1988**, *129*, 243.

(5) Álvarez, R. M. S.; Cutin, E. H.; Della Védova, C. O.; Mews, R.; Haist, R.; Oberhammer, H. *Inorg. Chem.* **2001**, *40*, 5188.

(6) Leibold, C.; Cutin, E. H.; Della Védova, C. O.; Mack, H.-G.; Mews, R.; Oberhammer, H. *J. Mol. Struct.* **1996**, *375*, 207.

(7) Mora Valdez, M. I.; Cutin, E. H.; Della Védova, C. O.; Mews, R.; Oberhammer, H. *J. Mol. Struct.* **2002**, *607*, 207.

(8) Haist, R.; Álvarez, R. M. S.; Cutin, E. H.; Della Védova, C. O.; Oberhammer, H. *J. Mol. Struct.* **1999**, *484*, 249.

(9) Oberhammer, H.; Glemser, O.; Klüver, H. *Z. Naturforsch.* **1974**, *29A*, 901.

(10) Cutin, E. H.; Della Védova, C. O.; Mack, H.-G.; Oberhammer, H. *J. Mol. Struct.* **1995**, *354*, 165.

(11) Trautner, F.; Cutin, E. H.; Della Védova, C. O.; Oberhammer, H. *J. Mol. Struct.* **1999**, *510*, 53.

(12) Robles, N. L.; Cutin, E. H.; Oberhammer, H. *J. Mol. Struct.* **2006**, *789*, 152.

(13) Höfer, R.; Glemser, O. *Z. Naturforsch.* **1975**, *30B*, 458.

(14) Sipachev, V. A. *THEOCHEM* **1985**, *121*, 143; Sipachev, V. A. *Adv. Mol. Struct. Res.* **1999**, *5*, 263; Sipachev, V. A. *NATO Science Series II: Mathematics, Physic, Chemistry* **2002**, *68*, 73.

(15) Frisch, M. J.; Trucks, G. W.; Schlegel, H. B.; Scuseria, G. E.; Robb, M. A.; Cheeseman, J. R.; Montgomery, J. A., Jr.; Vreven, T.; Kudin, K. N.; Burant, J. C.; Millam, J. M.; Iyengar, S. S.; Tomasi, J.; Barone, V.; Mennucci, B.; Cossi, M.; Scalmani, G.; Rega, N.; Petersson, G. A.; Nakatsuji, H.; Hada, M.; Ehara, M.; Toyota, K.; Fukuda, R.; Hasegawa, J.; Ishida, M.; Nakajima, T.; Honda, Y.; Kitao, O.; Nakai, H.; Klene, M.; Li, X.; Knox, J. E.; Hratchian, H. P.; Cross, J. B.; Bakken, V.; Adamo, C.; Jaramillo, J.; Gomperts, R.; Stratmann, R. E.; Yazyev, O.; Austin, A. J.; Cammi, R.; Pomelli, C.; Ochterski, J. W.; Ayala, P. Y.; Morokuma, K.; Voth, G. A.; Salvador, P.; Dannenberg, J. J.; Zakrzewski, V. G.; Dapprich, S.; Daniels, A. D.; Strain, M. C.; Farkas, O.; Malick, D. K.; Rabuck, A. D.; Raghavachari, K.; Foresman, J. B.; Ortiz, J. V.; Cui, Q.; Baboul, A. G.; Clifford, S.; Cioslowski, J.; Stefanov, B. B.; Liu, G.; Liashenko, A.; Piskorz, P.; Komaromi, I.; Martin, R. L.; Fox, D. J.; Keith, T.; Al-Laham, M. A.; Peng, C. Y.; Nanayakkara, A.; Challacombe, M.; Gill, P. M. W.; Johnson, B.; Chen, W.; Wong, M. W.; Gonzalez, C.; Pople, J. A. *Gaussian 03*; revision B.04; Gaussian, Inc.: Wallingford, CT, 2004.

(16) Álvarez, R. M. S.; Mora Valdez, M. I.; Cutin, E. H.; Della Védova, C. O. *J. Mol. Struct.* **2003**, *657*, 291.

(17) Álvarez, R. M. S.; Cutin, E. H.; Mack, H.-G.; Sala, O.; Della Védova, C.O. *J. Mol. Struct.* **1994**, *328*, 221.

(18) Boese, R.; Cutin, E. H.; Mews, R.; Robles, N. L.; Della Védova, C. O. *Inorg. Chem.* **2005**, *44*, 9660.

(19) Hamilton, W. C. *Acta Cryst.* **1965**, *18*, 502.

(20) Oberhammer, H. *Molecular Structure by Diffraction Methods*; The Chemical Society; London, 1976; Vol. 4, p 24.

(21) Atavin, E. G.; Vilkov, L. V. *Instruments and Experimental Techniques* (in Russian) 45 **2002**, 27.